Integrated and shared charging optimization of electric buses and shared micromobility incorporating solar photovoltaic

Downloaded from: https://research.chalmers.se, 2026-02-18 12:47 UTC

Citation for the original published paper (version of record):

Liu, X., Najafi, A., Jin, S. et al (2026). Integrated and shared charging optimization of electric buses and shared micromobility
incorporating solar photovoltaic. Transportation Research Part E: Logistics and Transportation Review, 208. http://dx.doi.org/10.1016/j.tre.2026.104709

N.B. When citing this work, cite the original published paper.

research.chalmers.se offers the possibility of retrieving research publications produced at Chalmers University of Technology. It covers all kind of research output: articles, dissertations, conference papers, reports etc. since 2004. research.chalmers.se is administrated and maintained by Chalmers Library

(article starts on next page)

Transportation Research Part E 208 (2026) 104709

Contents lists available at ScienceDirect

Transportation Research Part E

journal homepage: www.elsevier.com/locate/tre

Integrated and shared charging optimization of electric buses and shared micromobility incorporating solar photovoltaic

Xiaohan Liu [a], Arsalan Najafi [a], Sheng Jin [b], Hua Wang [c], Xiaolei Ma [d], Kun Gao [a,*]

[a] Department of Architecture and Civil Engineering, Chalmers University of Technology, Goteburg, SE-412 96, Sweden
[b] Institute of Intelligent Transportation Systems, College of Civil Engineering and Architecture, Zhejiang University, Hangzhou, 310058, China
[c] School of Automotive and Transportation Engineering, Hefei University of Technology, Hefei, 230009, China
[d] School of Transportation Science and Engineering, Beihang University, Beijing, 100191, China

ARTICLE INFO

Keywords:
Battery electric bus
shared charging
solar photovoltaic
charging infrastructure planning
charging scheduling
bi-level programming

ABSTRACT

Public transport electrification contributes to the net-zero goal in the transport sector. However, high-power bus charging during peak hours places additional strain on the grid, while under-utilization of charging infrastructure limits its potential economic and social benefits. This study focuses on these challenges through integrated and shared optimization of battery electric buses (BEB) and shared micromobility systems (SMS) incorporating solar photovoltaic. We present a bi-level mixed-integer linear programming model (B-MILM) to jointly optimize BEB charging infrastructure, BEB charging schedules, solar PV installed capacity, and SMS charging schedule. The B-MILM is solved using a value-function-based exact approach. We derive a group of inequalities based on the problem characteristics to reduce solution time. A large-scale case study in Gothenburg, Sweden, demonstrates that solar photovoltaic and shared charging services yield annual cost savings 110% - 120% above investment costs for public transit agencies, even when the service fee revenue is excluded. Charging dispatching costs for e-scooter operators are reduced by up to 54%, and daily BEB charging grid loads decrease by 3% to 34% across seasons. The greenhouse emissions from electricity consumption of BEBs and e-scooters are reduced by 3%. The results offer new insights for sustainable charging and energy infrastructure planning and management for electric public transit.

1. Introduction

Substantial efforts are being made to electrify public transport (PT) to align with the net-zero goal (He et al., 2025). In 2022, nearly 66,000 electric buses were sold globally (IEA, 2024). However, PT electrification faces two major challenges. First, the range anxiety associated with battery electric buses (BEBs) necessitates frequent high-power charging (McCabe et al., 2025), which stresses the power grid, particularly during peak-load hours. Second, since BEBs spend most of their time in service, the low charging infrastructure utilization restricts its potential economic and social benefits. Regarding these challenges, existing research has explored shared charging scheduling services by sharing BEB charging hubs for private cars (Ji et al., 2023; Jia et al., 2024) and ride-sourcing services (Cai et al., 2024). These studies commonly document increased benefits for involved stakeholders. Charging accessibility is improved

* Corresponding author.
E-mail addresses: xiaohanl@chalmers.se (X. Liu), arsalan.najafi@chalmers.se (A. Najafi), jinsheng@zju.edu.cn (S. Jin), hwang191901@hfut.edu.cn (H. Wang), xiaolei@buaa.edu.cn (X. Ma), gkun@chalmers.se (K. Gao).

https://doi.org/10.1016/j.tre.2026.104709
Received 14 May 2025; Received in revised form 5 January 2026; Accepted 19 January 2026
Available online 28 January 2026
1366-5545/© 2026 The Author(s). Published by Elsevier Ltd. This is an open access article under the CC BY license (http://creativecommons.org/licenses/by/4.0/).

for users of private cars and ride-sourcing services, while PT operators can gain additional revenues from shared charging modes. Additionally, a growing body of research investigates BEB charging infrastructure planning integrated with solar photovoltaic (PV) energy (Liu et al., 2024; Ren et al., 2022; Luo et al., 2024). These studies show that integrating solar PV at bus charging hubs can reduce charging costs and grid loads. Besides, existing studies also focus on the integrated optimization of BEB charging infrastructure and schedules to lower investment and charging costs while responding to time-of-use prices (He et al., 2022; Wang et al., 2023; Zhou et al., 2023, 2022b).

As the complementary travel modes to PT, shared micromobility systems (SMS), such as shared e-scooters and e-bikes, are popular low-carbon travel modes in urban areas (Li et al., 2024a). In the US alone, the National Association of City Transportation Officials reported 136 million shared micromobility trips in 2019 (NACTO, 2020). In Europe, more than 240 million trips by shared e-scooters were recorded in 2022 across 515 cities (MMfE, 2023). In the SMS system, an SMS charging point refers to a depot where the batteries of shared micromobility vehicles are recharged, while an SMS zone denotes a geographical area in which SMS staff operate battery-swapping trucks to transport depleted batteries to these charging points (Levy, 2024). Vehicle batteries are typically dispatched between SMS charging points and SMS zones, known as battery swapping. SMS charging points not only occupy urban land but also incur high battery dispatch costs, as urban planning frameworks limit the number of these points. Furthermore, the limited charging accessibility for SMS vehicles prevents timely battery charging, potentially reducing the level of service for customers due to concerns about riding range. Existing research has investigated battery swapping and vehicle re-balancing strategies for electric scooter sharing systems to improve the system service level (Lee et al., 2024; Osorio et al., 2021). Nevertheless, existing studies have not focused on the planning or operational challenges of sharing BEB charging hubs with SMS. Regarding integrating solar PV and bus charging infrastructure, the quantitative impacts still need to be understood in shared charging service modes. Therefore, this study aims to fill these gaps by investigating a BEB charging infrastructure planning and scheduling problem considering both SMS and solar PV adoption.

The contribution of this study is summarized as follows. Unlike existing research, new challenges arise when a SMS operator is incorporated into a BEB charging optimization problem. First, the interests of PT and SMS operators are not completely aligned. PT operators aim to maximize charging service revenues from SMS operators, while SMS operators minimize operational costs by optimizing SMS battery dispatching. For example, given the fixed service fee, PT operators might prefer assigning SMS batteries to the available bus charging hub deployed solar PV systems, even if it is far from the SMS zones, to maximize their revenue. In contrast, SMS operators prefer assigning batteries to nearby charging hubs to reduce dispatching costs. Hence, we formulate the problem as a bi-level mixed integer linear model (B-MILM) to minimize the overall system costs for PT operators in the upper-level problem and the operational costs for SMS operators in the lower-level problem. For PT operators, the decision variables include the number of chargers, solar PV installed capacity, and BEB charging schedules. For SMS operators, the decision variables are the battery dispatching schedules. The computational challenge of applying the developed B-MILM to city-scale instances arises due to the problem's complexity. To address this, we adopt a value-function-based exact approach. This approach iteratively solves the relaxation problem to obtain lower bounds and uncovers bilevel feasible solutions to obtain upper bounds (Lozano and Smith, 2017). We introduce variable-fixing strategies and additional inequalities derived from the problem's characteristics to strengthen the model formulation. Numerical instances demonstrate the positive effects of these techniques on solution efficiency. Finally, a city-scale case study is conducted in Gothenburg, Sweden, involving 70 bus routes, 705 buses, 61 bus terminals, and 12,000 shared e-scooters.

The rest of this paper is organized as follows: Section 2 reviews existing studies on bus charging infrastructure planning problems. Section 3 describes and formulates the problem. Section 4 introduces the value-function-based exact approach. Section 5 presents the algorithm's performance and a case study. Finally, Section 6 provides the conclusion and discusses future work.

2. Literature review

2.1. Related problem modeling

Given the mixed bus fleets (e.g., BEBs and diesel buses) at the early transition stage, studies focused on the bus charging infrastructure locations for mixed bus fleets (Li et al., 2021; Zhang et al., 2022; Cui et al., 2023). Mixed bus fleets involve heterogeneous refueling constraints and long-term bus fleet transition decisions. Li et al. (2021) presented a space-time-state (energy) network to formulate a two-stage stochastic programming model for optimizing bus charging hub locations and charging schedules. The bus service network in their study considers diesel buses and BEBs, including fixed bus schedules and ad hoc services. The case study in Hong Kong demonstrates the advantages of the space-time-state network formulation and reliability-based gradient algorithm. With the advancement of charging technologies, extensive studies investigated alternative charging technologies besides chargers, such as battery swapping (Huang et al., 2023), wireless charging infrastructure (Li et al., 2024b), and opportunity charging based on ultra chargers (Wang et al., 2023). This charging infrastructure requires problem modeling by incorporating bus charging scheduling at the single-vehicle level. For instance, Li et al. (2024b) investigated a bus charging infrastructure planning problem by introducing dynamic wireless charging technology. A mixed integer nonlinear programming model is formulated to minimize the sum of charging infrastructure, BEB battery, and BEB charging costs. The case study shows the economic benefits of deploying dynamic wireless charging infrastructure under specific assumptions and scenarios. Regarding the problem's uncertain factors, such as energy consumption and travel time, two-stage robust stochastic optimization models could be established to minimize the total cost under uncertain conditions (Wang et al., 2024). In the first stage, deterministic decisions, such as charging infrastructure locations and capacity, are made, while the second stage determines bus charging schedules under uncertain conditions, which are captured by specific uncertainty sets. Another study presents a prediction and optimization framework to address the uncertainty in vehicle arrival

times and charging demand (Mahyari et al., 2023). In their work, a machine learning-based prediction model is incorporated into the optimization process, and the charging scheduling problem is solved using a rolling-horizon online optimization approach.

In recent years, a growing body of research has investigated integrating solar PV systems into bus charging infrastructure planning. Based on the bus charging hubs or bus depots, PV panels can be installed on the rooftops of buildings at or near the depots. To evaluate the potential of solar PV power outputs, a 3D-GIS-based framework can be used to estimate the solar PV power outputs by considering shading impacts (Ren et al., 2022). Additionally, one study proposed a two-stage stochastic optimization model to account for the uncertainty of solar PV power outputs (Liu et al., 2023b). To highlight the grid power degradation during extreme weather, a study develops a two-stage robust optimization model utilizing solar PV energy to offset the electricity needed for charging BEBs (Liu et al., 2023a). Jointly planning the PT system, energy network, and distributed solar PV offers a systemic solution for sustainable urban transportation. One study presented a three-level programming model for the coupled transportation and energy systems (Luo et al., 2024). Regarding optimizing the solar PV deployment across the entire bus network, Liu et al. (2024) proposed a data-driven optimization framework by integrating multiple datasets, such as bus GPS trajectory data, weather data, and bus depot building information. The original solar PV deployment problem is decomposed into independent sub-problems based on the single bus depot. The case study in Beijing shows that introducing solar PV could reduce the net grid loads of bus charging and yield obvious economic benefits.

2.2. Related solution approaches

The solution approaches to the optimization models depend on the model structure and the types of objectives, constraints, and parameters. The nonlinear constraints could be reformulated as linear forms to solve the mixed integer programming models. For example, the approximated linear charging functions and battery degradation could be incorporated in the models (Zhou et al., 2022a). When vehicle-trip matching is integrated into the bus charging, the off-the-shelf solvers could solve small-scale instances directly. However, it could fail to solve the middle and large-scale instances directly using solvers. In this case, heuristics and surrogate-based optimization methods could be employed to find near-optimal solutions (Foda et al., 2023; Nath et al., 2024). When the optimization models involve uncertain parameters (e.g., energy consumption and travel time), robust or stochastic optimization models are usually required. Such optimization models could be transformed into deterministic formulations using robust or stochastic optimization techniques (e.g., budget uncertainty sets and progressive hedging) (Alwesabi et al., 2022; Esmaeilnejad et al., 2023). This study is different from the existing studies regarding problem modeling and solving. First, we present a bi-level mixed integer linear programming model considering the game process between PT and SMS operators. We also present a novel problem combination incorporating bus charging, SMS battery dispatching, shared charging mode, and solar PV. Regarding the solution approach, we adopt a value-function-based approach and present tailored inequalities to solve this complex problem exactly and effectively.

3. Model formulation

This section first describes the problem and introduces the sets, parameters, and decision variables used in the model. Next, the details of the B-MILM are presented. Finally, variable-fixing strategies are proposed to strengthen the model formulation.

3.1. Problem statement

In this problem, bus routes, bus terminals, bus schedules, SMS zones, SMS charging points, and SMS charging demand are defined and fixed as inputs. Bus schedules are derived from the information on the timetables, considering the number of buses used and their state-of-charge (SoC). Since this study focuses specifically on the problem of charging scheduling and infrastructure planning based on given bus schedules, the details of bus schedule generation are not presented in this paper. Bus terminals are designated as potential bus charging hubs equipped with chargers. In the following text, “bus terminal” consistently refers to “bus charging hub”. Solar PV systems can be deployed at these hubs, with their installed capacity determined within the model. SMS operators can dispatch SMS batteries using electric mini-trucks between SMS zones and SMS charging points or bus charging hubs. For simplicity, we refer to the PT operator as the leader and the SMS operator as the follower. The leader variables include the number of chargers, installed capacity of solar PV, and BEB charging schedules, while the follower variables are battery dispatching schedules. The follower must make decisions based on the leader’s decisions, and the leader must consider the follower’s response when making decisions. We assume that the electric mini-trucks have sufficient capacity to transport scheduled SMS batteries between SMS zones and the charging infrastructure. In each SMS zone, a SMS staff member operates an electric mini-truck. SMS batteries should be charged when their SoC falls below 20%. SMS charging demands can be estimated using SMS transaction data and must be met hourly within each SMS zone. We assume that each SMS charging event at bus charging hubs incurs a service fee. This fee includes only the charging-resource occupancy component and excludes the electricity cost associated with SMS charging at bus hubs. In addition, the PT operator receives payment for the electricity purchased by SMS at the utility market price, regardless of whether the electricity is supplied by the grid or by on-site solar PV. Consequently, the net profit from SMS charging for BEB operators has two components: (i) the service fee and (ii) the electricity-payment revenue corresponding to the portion of SMS charging demand supplied by on-site PV generation. In other words, SMS users pay for the full energy consumed at the utility market price, while the operator’s net revenue arises from the PV-supplied energy that does not need to be gained from the grid. Fig. 1 illustrates the cooperation relationship diagram between SMS and PT operators. Green lines indicate revenue or cost-saving flows, whereas red lines denote costs paid.

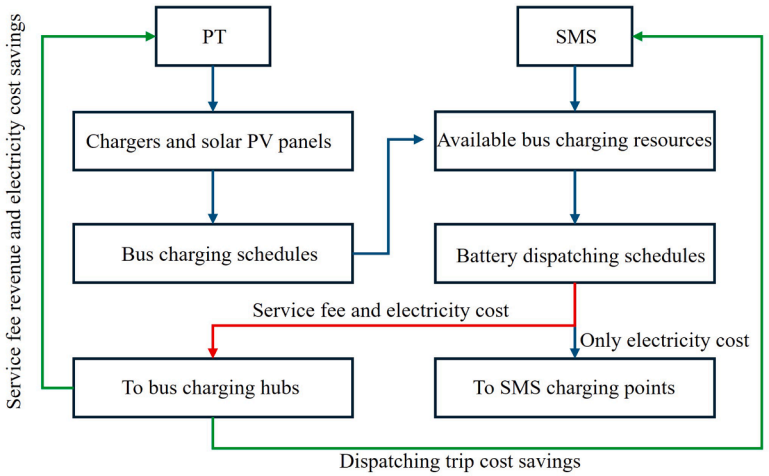

Fig. 1. Cooperation relationship diagram between SMS and PT operators.

To assess the feasibility of sharing charging resources with SMS, it is essential to understand the charging patterns of electric buses. Electric buses typically employ two primary charging strategies: depot charging and opportunity charging (Jia et al., 2024). Depot charging involves recharging buses in centralized facilities during off-peak hours, often overnight, using a low charging rate. Therefore, the unoccupied charging capacity could be shared with SMS. Opportunity charging refers to the practice of recharging electric buses at bus charging stations with fast chargers during layover periods between trips. Based on GPS trajectory data from over 20,000 buses in Beijing, only 22% of the fleet are simultaneously stationed at depots during daytime hours (Liu et al., 2024). Therefore, there is potential to share bus charging capacities with SMS, even when employing an opportunity charging strategy.

We assume the presence of advanced SMS battery assembly systems capable of integrating multiple SMS battery modules into containerized units transportable by mini-trucks. These containers can be charged in parallel by exploiting the unused charging capacity at bus charging hubs. For instance, a container comprising 20 SMS batteries with an aggregate charging power of 22 kW could be fully charged within 30 minutes. Fully utilizing the residual charging capacity of bus charging hubs is thus crucial for system efficiency. Several SMS companies employ battery-swapping systems and utilize compact charging cabinets at their service points (Shared micromobility, 2021). Such cabinets can be integrated into trucks or installed at bus charging hubs, occupying as little as 2 m^2 of space.

Although several SMS companies have deployed some advanced SMS chargers (which integrate docking and charging functions for SMS vehicles) along streets in the SMS market, this type of charging and service model limits the feasibility of SMS. Table 1 presents the sets, parameters, and decision variables used in the model.

3.2. Bi-level mixed integer linear model

3.2.1. Leader problem

The leader problem is formulated as a mixed integer linear programming model. The objective function and constraints are written as follows.

$$\min \sum_{j\in J_B} C_{PV} S_j + \sum_{j\in J_B} C_{CH} N_j + \sum_{h\in H} \theta_h \sum_{v\in V} \sum_{k\in K_v} \sum_{t_0\in T^0} \lambda_{t_0} \sum_{t\in T_{t_0}^{sub}} r_{hvkt} - \sum_{h\in H} \theta_h \sum_{j\in J_B} \sum_{t_0\in T^0} \lambda_{t_0} u_{hjt_0} - C_{fee} \sum_{h\in H} \theta_h \sum_{i\in I} \sum_{j\in J_B} \sum_{t_0\in T^0} o_{h,ij,t_0,B} \tag{1}$$

$$E_{h,v,k}{}' = E'_{h,v,k-1} - e_{vkh} + \sum_{t\in T} r_{hvkt}, \forall h \in H, v \in V, k \in K_v \tag{2}$$

$$E'_{h,v,k-1} - e_{vkh} \geq SoC_{\min} C_v, \forall h \in H, v \in V, k \in K_v \tag{3}$$

$$E'_{h,v,k} \leq C_v, \forall h \in H, v \in V, k \in K_v \tag{4}$$

$$E'_{h,v,0} = C_v, \forall h \in H, v \in V \tag{5}$$

Table 1
The model notions of sets, indices, parameters, and decision variables.

Sets (indices)	Description
T (t)	Sets of 20 minutes for a day.
T^0 (t_0)	Sets of hours for a day.
$T^{sub}_{t_0}$ (t)	Sets of 20 minutes in hour t_0.
H (h)	Sets of seasonal scenarios regarding solar PV power outputs.
V (v)	Sets of BEBs in an electric PT network.
K_v (k)	Sets of daily trips of BEB v.
J_B (j)	Sets of bus terminals (Potential bus charging hubs).
J_E (j)	Sets of existing SMS charging hubs.
I (i)	Sets of SMS zones.
Parameters	**Description**
C_{PV}	Annual investment for the unit installed capacity of solar PV (US$/kW).
C_{CH}	Annual investment of a charger (US$).
C_{fee}	Service fee charged by the PT operator to SMS for each battery charging event, corresponding to the charging-resource occupancy at a bus charging hub (US$).
θ_h	Number of days in seasonal scenario h.
λ_{t_0}	Utility electricity price in hour $t_0 \in T^0$ (US$/kWh).
e_{vkh}	Electricity consumption of BEB v in trip k in seasonal scenario h (kWh).
$SoC_{\min}$	Minimum allowable SoC of BEBs (20% in this study).
C_v	Battery capacity of BEB v (kWh).
p	Maximum charging power of a charger (kW).
Δ_{vkt}	Occupied layover time of BEB v after trip k in time interval $t \in T$ (hour).
δ_{vkjt}	1 if BEB v after trip k at bus terminal j of time interval $t \in T$ and 0 otherwise.
e	Averaged charging demand of a SMS battery (kWh).
d_{it_0}	Number of SMS batteries needing to be charged in SMS zone i in hour $t_0 \in T^0$.
g_{ht_0}	Solar PV power of scenario h in hour $t_0 \in T^0$ for the unit installed capacity (kW).
$S_{j,\max}$	Maximum allowable installed capacity at bus terminal j (kW).
$N_{j,\max}$	Maximum allowable number of chargers deployed at bus terminal j.
C_{ij}	Operational cost of a SMS battery dispatching trip from i to j (including the electricity consumption cost of an electric mini-truck, labor cost, and half of the service fee) (US$).
Δt	Duration of time intervals for all t belongs to T (20 minutes in this study).
Leader variables	**Description**
S_j	Installed capacity of solar PV at bus terminal j (kW).
N_j	Number of chargers deployed at bus terminal j.
$E'_{h,v,k}$	SoC of BEB v after trip k and after possible charging and before the next trip in scenario h (kWh).
u_{hjt_0}	Amount of used solar PV electricity at bus terminal j in hour $t_0 \in T^0$ in scenario h (kWh).
r_{hvkt}	Electricity charged for BEB v after trip k in time interval $t \in T$ in scenario h (kWh).
z_{hvkt}	1 if BEB v is charged after trip k in time interval $t \in T$ in scenario h and 0 otherwise.
Follower variables	**Description**
$o_{h,ij,t_0,E}$	1 if SMS batteries are dispatched from zone i to SMS charging point j in hour $t_0 \in T^0$ in scenario h and 0 otherwise.
$o_{h,ij,t_0,B}$	1 if SMS batteries are dispatched from zone i to bus charging hub j in hour $t_0 \in T^0$ in scenario h and 0 otherwise.

$$E'_{h,v,|K_v|} = C_v, \forall h \in H, v \in V \tag{6}$$

$$r_{hvkt} \le p\Delta_{vkt} z_{hvkt}, \forall h \in H, v \in V, k \in K_v, t \in T \tag{7}$$

$$\sum_{v \in V} \sum_{k \in K_v} \delta_{vkjt} z_{hvkt} \le N_j, \forall h \in H, j \in J_B, t \in T \tag{8}$$

$$u_{hjt_0} \le \min\{ \sum_{v \in V, k \in K_v, t \in T^{sub}_{t_0}} \delta_{vkjt} r_{hvkt} + e \sum_{i \in I} d_{it_0} o_{h,ij,t_0,B}, g_{ht_0} S_j \}, \forall h \in H, j \in J_B, t_0 \in T^0 \tag{9}$$

$$0 \le S_j \le S_{j,\max}, \forall j \in J_B \tag{10}$$

$$0 \le N_j \le N_{j,\max}, N_j \in \mathbb{Z}, \forall j \in J_B \tag{11}$$

$$E'_{h,v,k} \ge 0, \forall h \in H, v \in V, k \in K_v \tag{12}$$

$$u_{hjt_0} \ge 0, \forall h \in H, j \in J_B, t_0 \in T^0 \tag{13}$$

$$r_{hvkt} \ge 0, \forall h \in H, v \in V, k \in K_v, t \in T \tag{14}$$

$$z_{hvkt} \in \{0,1\}, \forall h \in H, v \in V, k \in K_v, t \in T \tag{15}$$

Objective (1) minimizes the sum of the solar PV investment, charger investment, BEB charging costs, and charging revenues from SMS (treated as negative costs). Let C_{PV} and C_{CH} denote the annual investments for the installed solar PV unit capacity and per charger, respectively. Let C_{fee} denote the service fee charged by the PT to the SMS for a single battery charging event at a bus charging hub. We use θ_h to denote the number of days in scenario h. Let λ_{t_0} denote the hourly utility electricity price in hour t_0. Let S_j indicate the installed capacity of solar PV at bus terminal j. Let N_j denote the number of chargers deployed at bus terminal j. We use r_{hvkt} to denote the electricity charged for BEB v after trip k in time interval t in scenario h. Let u_{hjt_0} denote the amount of used solar PV electricity at bus terminal j in hour t_0 in scenario h. Let $o_{h,ij,t_0,B}$ denote a binary follower variable: 1 if SMS batteries are dispatched from zone i to bus charging hub j in hour $t_0 \in T^0$ in scenario h and 0 otherwise. Constraints (2)–(6) ensure the SoC of BEB batteries remains between 20% and 100%. Here, let $E'_{h,v,k}$ represent the SoC of BEB v after trip k and after any possible charging and before the next trip in scenario h. Let e_{vkh} denote the electricity consumption of BEB v in trip k in seasonal scenario h. Let $SoC_{\min}$ equal 20%, indicating the minimum allowable SoC of BEBs. C_v denotes the battery capacity of BEB v. Constraint (7) reveals that the amount of charged electricity for BEBs does not exceed the electricity supply capacity, where p represents the maximum charging power of chargers and Δ_{vkt} indicates the occupied layover time of BEB v after trip k in time interval t. Each time interval has a duration of 20 minutes. The time interval in this model represents only the periods during which charging resources are occupied or unoccupied. A duration of 20 minutes per interval is deemed appropriate for the desired modeling resolution. If the interval is too short, the computational time increases significantly. If it is too long, the charging resources may be underutilized. Constraint (7) also indicates that a charger will be occupied if a BEB is being charged at the bus charging hub. Let z_{hvkt} denote a binary variable: 1 if BEB v is charged after trip k in time interval t in scenario h and 0 otherwise. Constraint (8) guarantees that the number of chargers occupied at any given time does not exceed the number of chargers deployed. Let δ_{vkjt} equal 1 if BEB v after trip k at bus terminal j of time interval t and otherwise 0. Constraint (9) ensures that the amount of solar PV electricity used does not exceed the combined charging demand of PT and SMS, nor does it exceed the solar PV energy production. We use e to denote the averaged charging demand of a SMS battery. Let d_{it_0} denote the number of SMS batteries needing to be charged in SMS zone i in hour t_0. We use $o_{h,ij,t_0,B}$ to indicate a binary variable: 1 if SMS batteries are dispatched from zone i to bus charging hub j in hour t_0 in scenario h and 0 otherwise. Let g_{ht_0} represent solar PV power of scenario h in hour t_0 for the unit installed capacity. In particular, we use $t \in T^{sub}_{t_0}$ in Constraint (9) to denote the index (t) of the 20-minute intervals within hour t_0. The aggregated 20-minute charging demand of the PT system in hour t_0 is then allocated to the hourly time resolution. Constraints (10)–(15) define the variable ranges. Let $S_{j,\max}$ denote the maximum allowable installed capacity at bus terminal j. We use $N_{j,\max}$ to indicate the maximum allowable number of chargers deployed at bus terminal j.

Notably, we model BEB charging using a 20-minute time resolution in this study. Although prior studies have addressed related problems using a 1-minute resolution (Abdelwahed et al., 2020; Caustur et al., 2025), adopting such a fine granularity within our bi-level framework would lead to a computational burden. In general, increasing the time resolution enlarges the feasible solution space and can improve model accuracy, but it also imposes an exponentially growing computational burden. In this study, we consider both the battery capacity of BEBs and the charging power of fast chargers. Balancing the trade-off between model accuracy and computational complexity, we adopt a 20-minute time resolution, as it typically corresponds to an average charging duration under realistic battery capacities and charging power levels.

3.2.2. Follower problem

The follower problem is formulated as a binary linear programming model. The objective function and the constraints are presented below.

$$\min \sum_{h\in H} \theta_h \sum_{i\in I} \sum_{j\in J_B} \sum_{t_0\in T^0} 2C_{ij} o_{h,ij,t_0,B} + \sum_{h\in H} \theta_h \sum_{i\in I} \sum_{j\in J_E} \sum_{t_0\in T^0} 2C_{ij} o_{h,ij,t_0,E} \tag{16}$$

$$\sum_{j\in J_E} o_{h,ij,t_0,E} + \sum_{j\in J_B} o_{h,ij,t_0,B} \le 1, \forall h \in H, i \in I, t_0 \in T^0 \tag{17}$$

$$d_{it_0}\Big(\sum_{j\in J_E} o_{h,ij,t_0,E} + \sum_{j\in J_B} o_{h,ij,t_0,B} - 1\Big) \ge 0, \forall h \in H, i \in I, t_0 \in T^0 \tag{18}$$

$$\sum_{j\in J_E} o_{h,ij,t_0,E} + \sum_{j\in J_B} o_{h,ij,t_0,B} \le d_{it_0}, \forall h \in H, i \in I, t_0 \in T^0 \tag{19}$$

$$e\sum_{i\in I} d_{it_0} o_{h,ij,t_0,B} \le N_j p - \sum_{v\in V} \sum_{k\in K_v} \sum_{t\in T^{sub}_{t_0}} \delta_{vkjt} z_{hvkt} p\Delta t, \quad \forall h \in H, j \in J_B, t_0 \in T^0 \tag{20}$$

$$o_{h,ij,t_0,B} \in \{0,1\}, \forall h \in H, i \in I, j \in J_B, t_0 \in T^0 \tag{21}$$

$$o_{h,ij,t_0,E} \in \{0,1\}, \forall h \in H, i \in I, j \in J_E, t_0 \in T^0 \tag{22}$$

Objective (16) minimizes the SMS battery dispatching cost, where C_{ij} represents the operational cost (involving the electricity consumption cost of an electric mini-truck, labor cost, and half of the service fee) of a SMS battery dispatching trip from i to j. We use $o_{h,ij,t_0,E}$ to indicate a binary variable: 1 if SMS batteries are dispatched from zone i to SMS charging point j in hour t_0 in scenario h and 0 otherwise. The coefficient of 2 in the second term represents the costs of round-trip trips between SMS zones and charging sites. Constraint (17) ensures that SMS batteries are dispatched by no more than one electric mini-truck to a single charging location per hour for each SMS zone. Constraints (18) and (19) specify that SMS batteries must be dispatched and charged if there is a charging need; otherwise, they should not be dispatched. Constraint (20) reveals that SMS batteries should be charged using idle chargers at the bus charging hubs. Here, we use Δt to denote a fixed time interval of 20 minutes. We also use $t \in T_{t_0}^{sub}$ to denote the index (t) of the 20-minute intervals within hour t_0. The aggregated 20-minute charging demand of the PT system in hour t_0 is then allocated to the hourly time resolution. Thus, SMS batteries should not be dispatched to bus charging hubs where the charging supply cannot meet the SMS charging demands. Constraints (21) and (22) define binary follower variables.

3.2.3. Variable fixing

The number of follower variables increases with the number of bus charging hubs, SMS charging points, and SMS zones. Consequently, applying the B-MILM to city-scale instances will result in significant computational burdens. To address this concern, a variable-fixing strategy is employed to reduce the feasible solution space of follower variables. For SMS zone i, only SMS charging points with minimum cost coefficients could be retained as the feasible SMS charging points. Additionally, for SMS zone i, any bus charging hub with a cost coefficient exceeding the minimum cost coefficient among the SMS charging points is considered an infeasible dispatching option for that zone. Our model assumption is reasonable under real-world conditions. We focus on the bus charging infrastructure planning problem within a context where SMS charging points are already well-established. Consequently, each SMS charging point must meet the charging demands of the nearby zones. Therefore, this study does not consider the power capacity issues for SMS charging points.

4. Value-function-based exact solution approach

4.1. Extended high point problem

For simplicity, we use $\phi^l(x^l, x^f)$ to denote objective function (1) where x^l and x^f represent the leader and follower variables, respectively. We also use $\phi^f(x^l, x^f)$ denote objective function (16). Let $\Omega = \{(x^l, x^f)\}$ indicate the feasible set of (x^l, x^f) regarding Constraints (2)–(15) and (17)–(22). Here, we define a high-point problem as follows.

$$\chi_{HPP} = \min \phi^l(x^l, x^f), \forall (x^l, x^f) \in \Omega \tag{23}$$

The solution to HPP provides a lower bound of the original problem. Given x^l, we define $y(x^l) = \{x^f\}$, which meets Constraints (17)–(22). The value-function-based solution approach reformulates the original model as an extended high point problem (EHPP). The EHPP extends the HPP by introducing new constraints. The new constraints can enforce the bilevel feasibility conditions, meaning that the leader's decisions must be made with respect to the optimal response from followers. To achieve this, for every $\hat{x}^f$ in y, the leader should either choose a (x^l, x^f) such that $\phi^f(x^l, x^f) \le \phi^f(x^l, \hat{x}^f)$ where $\hat{x}^f \in y(x^l)$, or block $\hat{x}^f$ to belong to $y(x^l)$ by selecting such a x^l. Obviously, if $\hat{x}^f$ does not belong to $y(x^l)$, it is not necessary to ensure $\phi^f(x^l, x^f) \le \phi^f(x^l, \hat{x}^f)$. Let $g(x^l)$ denote the terms associated with the leader variables in Constraint (20) below.

$$g_{hjt_0}(x^l) = -N_j p + \sum_{v \in V} \sum_{k \in K_v} \sum_{t \in T_{t_0}^{sub}} \delta_{vkjt} z_{hvkt} p \Delta t, \forall h \in H, j \in J_B, t_0 \in T^0 \tag{24}$$

Let $w(x^f)$ denote the terms associated with the follower variables in Constraint (20) as follows.

$$w_{hjt_0}(x^f) = e \sum_{i \in I} d_{it} o_{h,ij,t_0,B}, \forall h \in H, j \in J_B, t_0 \in T^0 \tag{25}$$

To write the EHPP explicitly, we introduce the following auxiliary parameters and sets.

$$\gamma_{\hat{x}^f,hjt_0} = \lfloor -w_{hjt_0}(\hat{x}^f) \rfloor + 1, \forall \hat{x}^f \in y, h \in H, j \in J_B, t_0 \in T^0 \tag{26}$$

$$B(\hat{x}^f, y) = \{(x'^f, h, j, t_0) | \gamma_{x'^f,hjt_0} \ge \gamma_{\hat{x}^f,hjt_0}, x'^f \in y, h \in H, j \in J_B, t_0 \in T^0\} \tag{27}$$

The leader can block $\hat{x}^f$ to belong to $y(x^l)$ by Constraint (20) associated with h, j, and t_0 if and only if $g_{hjt_0}(x^l) \ge \gamma_{\hat{x}^f,hjt_0}$. For detailed proof, readers can reference Proposition 2 in Lozano and Smith's study (Lozano and Smith, 2017). The set $B(\hat{x}^f, y)$ includes all ordered tuples (x'^f, h, j, t_0) such that if a x^l blocks a $x'^f \in y(x^l)$ by Constraint (20) associated with h, j, and t_0, then this x^l also blocks $\hat{x}^f \in y(x^l)$. Based on the introduced auxiliary parameters and sets, the EHPP is formulated as follows.

$$\chi_{EHPP} = \min \phi^l(x^l, x^f) \tag{28}$$

$$g_{hjt_0}(x^l) \ge -M^1_{hjt_0} + \sum_{\hat{x}^f \in y} (M^1_{hjt_0} + \gamma_{\hat{x}^f,hjt_0}) \omega_{\hat{x}^f,hjt_0}, \forall h \in H, j \in J_B, t_0 \in T^0 \tag{29}$$

$$\phi^f(x^l, x^f) \le \phi^f(x^l, \hat{x}^f) + M^2 \sum_{(x'^f, h, j, t_0) \in B(\hat{x}^f, y)} \omega_{x'^f, hjt_0}, \forall \hat{x}^f \in y \tag{30}$$

$$(x^l, x^f) \in \Omega \tag{31}$$

$$\omega_{\hat{x}^f, hjt_0} \in \{0, 1\}, \forall \hat{x}^f \in y, h \in H, j \in J_B, t_0 \in T^0 \tag{32}$$

Objective (28) aligns with Objective (1) in the leader problem. Constraints (29) and (30) use binary auxiliary variable $\omega_{\hat{x}^f, hjt_0}$ to ensure bi-level feasibility condition, where $\omega_{\hat{x}^f, hjt_0} = 1$ if Constraint (29) associated with h, j, and t_0 blocks $\hat{x}^f \in y(x^l)$ and 0 otherwise. In particular, Constraint (29) is responsible for blocking the follower variables, while Constraint (30) ensure that $\phi^f(x^l, x^f) \le \phi^f(x^l, \hat{x}^f)$ unless $\hat{x}^f$ is blocked. According to Eq. (24), $g_{hjt_0}(x^l)$ is no less than $-N_j p$. This implies that $M^1_{hjt_0}$ can be set to the estimated number of chargers required multiplied by the power p. In this way, we can first determine the optimal number of chargers at the bus charging station without considering the SMS. Then, we set the estimated number of chargers to the optimal value augmented by an appropriate margin. Constraint (30) indicates that M^2 can be set to the maximum value of the objective function in the follower problem. The EHPP is equivalent to the B-MILM. For detailed proof, readers can reference Propositions 1, 2, and 3 in Lozano and Smith (2017). Appendix A presents the detailed description of EHPP.

4.2. Algorithm and convergence

In EHPP, enumerating all $\hat{x}^f \in y$ in Constraints (29) and (30) is impractical due to the curse of dimensionality. Even if all $\hat{x}^f \in y$ are enumerated, the binary auxiliary variable $\omega_{\hat{x}^f, hjt_0}$ associated with $\hat{x}^f$ could increase the computational burdens largely. Therefore, the EHPP is solved exactly using an iteration-based algorithm. The iteration-based algorithm starts with solving the HPP and extends the HPP to a restricted extended high point problem (REHPP) using the samples of $\hat{x}^f$. The number of samples increases as optimal follower solutions are included iteratively.

It should be noted that there are three assumptions that guarantee the exactness and convergence of the proposed algorithm by Lozano and Smith (2017). The first assumption states that both the upper- and lower-level feasible regions are compact sets. Obviously, the variables in our proposed model meet this assumption and have optimal solutions. The second assumption is that the terms involved leader variables in the follower problem should be integer valued. In our model, given the duration of the interval (20 minutes in this study), this assumption could be guaranteed if the maximum charging power is divisible by 3. The third assumption states that all leader variables are integer-valued. In our model, some of the leader variables are continuous, but the leader variables involved in the follower problem are integers. Proposition 1 will show that Algorithm 1 provides an optimal solution to the B-MILM within a finite number of iterations.

Algorithm 1 An iteration-based exact algorithm for the proposed B-MILM.

Require: Let $\tau = 0$. Let the sample set y_τ equals Φ. Initialize upper bound (UB_τ) to be $+\infty$ and lower bound (LB_τ) to be $\chi_{\tau,HPP}$.
Ensure: The optimal solution.

1: **while** $LB_\tau \le UB_\tau$ **do**
2: $\tau = \tau + 1$
3: Obtain an optimal solution (x^l_τ, x^f_τ) to REHPP(y_τ), and set $LB_\tau = \chi_{\tau,REHPP}$
4: Obtain an optimal solution $x^{f,FOLL}_\tau$ to the follower problem, and set $y_\tau = y_\tau \cup x^{f,FOLL}_\tau$.
5: **if** $\phi^f(x^l_\tau, x^{f,FOLL}_\tau) = \phi^f(x^l_\tau, x^f_\tau)$ **then**
6: Update $UB_\tau = LB_\tau$, and the optimal solution to the proposed B-MILM is obtained.
7: **else**
8: Let $u_{hjt_0,\tau} = \min(\sum_{v\in V}\sum_{k\in K_v}\sum_{t\in T^{sub}_{t_0}}\delta_{vkjt} r_{hvkt,\tau} + e\sum_{i\in I} d_{it_0} o^{FOLL}_{h,ij,t_0,B,\tau}, g_{ht_0} S_{j,\tau})$ to adjust x^l_τ. Let $UB_\tau = \min(UB_{\tau-1}, \phi^l(x^l, x^{f,FOLL}_\tau))$.
9: **end if**
10: **end while**

Proposition 1. *Algorithm 1 terminates and provides an optimal solution to the B-MILM within a finite number of iterations.*

Proof. The optimal solution of the current REHPP in Algorithm 1 represents a current lower bound of EHPP. When Algorithm 1 terminates, it indicates that the current lower bound of EHPP reaches its upper bound. Thus, under this condition, Algorithm 1 finds an optimal solution to EHPP. Since the two problems are equivalent, the optimal solution to the EHPP must also be the optimal solution to the B-MILM. Now, we show that Algorithm 1 terminates within a finite number of iterations. Observe that only N_j and z_{hvkt} are involved in the follower problem. The space of N_j and z_{hvkt} must be finite because they are discrete variables and are limited by the given bounds. Suppose that Algorithm 1 terminates after $|\Omega(N, z)| + 1$ iterations. There must be two iterations τ and τ', where $1 \le \tau \le \tau' \le |\Omega(N, z)| + 1$, such that $(N_\tau, z_\tau) = (N_{\tau'}, z_{\tau'})$. In line 4 of Algorithm 1, we obtain an optimal follower response $x^{f,FOLL}_\tau$. Since $\tau < \tau'$, we have $x^{f,FOLL}_\tau \in y_{\tau'}$. Since $x^{f,FOLL}_\tau$ represents the optimal solution to the follower problem given (N_τ, z_τ) and $x^{f,FOLL}_\tau \in y_{\tau'}$, Constraint (30) guarantees that $\phi^f(x^l_{\tau'}, x^f_{\tau'}) \le \phi^f(x^l_{\tau'}, x^{f,FOLL}_{\tau'})$, and we also have $(N_\tau, z_\tau) = (N_{\tau'}, z_{\tau'})$. This implies that $x^f_{\tau'}$ must be the optimal solution to the follower problem given $(N_{\tau'}, z_{\tau'})$, and Algorithm 1 reaches line 6 and terminates. Since

there must be two iterations τ and τ' such that $(N_\tau, z_\tau) = (N_{\tau'}, z_{\tau'})$ within $|\Omega(N,z)|+1$ iterations, Algorithm 1 always terminates within a finite number of iterations. □

4.3. Strengthening the REHPP formulation

Proposition 1 shows that Algorithm 1 can terminate within $|\Omega(N,z)|+1$ iterations. However, $|\Omega(N,z)|$ is extremely huge when the problem scale is at the city level. For each iteration, solving REHPP is also time-consuming. Therefore, it is necessary to accelerate the iteration procedure of Algorithm 1. There are two ways to accelerate the iteration procedure. The first way is to improve the solution efficiency for the REHPP by modifying or reformulating the REHPP. The second way is to find the two iterations τ and τ' such that $(N_\tau, z_\tau) = (N_{\tau'}, z_{\tau'})$ within a small number of iterations by strengthening the REHPP formulation. This paper focuses on the second way to accelerate the iteration procedure.

Definition 1. The inequalities are considered super valid if they can exclude some feasible or even optimal solutions for the current REHPP, while maintaining bi-level feasibility and optimality for the B-MILM.

Observation 1. *For the optimal follower's response, given the leader's decisions, the follower always assigns SMS batteries from a zone to either the SMS charging points or bus charging hubs with the least cost, provided that the available infrastructure can meet the SMS charging demand from this SMS zone.*

Observation 1 is straightforward and serves as a necessary condition for an optimal follower's response. Let I^0 represent the set of SMS zones where there exists at least one bus charging hub with lower operational costs for dispatching SMS batteries between the SMS zone and the bus charging hub compared with SMS charging points. Let J_{B,i^0} denote the set of bus charging hubs with lower operational costs for SMS zone $i^0 \in I^0$ for dispatching SMS batteries between the SMS zone and the bus charging hub compared with SMS charging points. For SMS zone $i^0 \in I^0$ and bus charging hub $j \in J_{B,i^0}$, let $U(i^0, j)$ denote the set of bus charging hubs where the charging hub belongs to J_{B,i^0} and the operational cost between SMS zone $i^0 \in I^0$ and this bus charging hub is higher than that associated with bus charging hub $j \in J_{B,i^0}$. Let $j_{i^0,E}$ denote the SMS charging point with the lowest operational cost for SMS zone $i^0 \in I^0$. We introduce a binary auxiliary variable $\pi_{hi^0jt_0}$ to linearize the logic relationship. In Constraint (33), M^3 could be set to $N_j p$. According to Constraint (17), the minimum value of the left side of Constraint (34) should be -1. Hence, we set M^4 to 1.

Now, we propose the super-valid inequalities according to Observation 1.

Proposition 2. *The following inequalities are super valid according to Definition 1.*

$$N_j p - \sum_{v\in V}\sum_{k\in K_v}\sum_{t\in T^{sub}_{t_0}} \delta_{vkjt} z_{hvkt} p\Delta t - e(d_{i^0t_0} + \sum_{i\in I\setminus i^0} d_{it_0} o_{h,ij,t_0,B}) \le M^3 \pi_{hi^0jt_0},$$
$$\forall h\in H, i^0\in I^0, j\in J_{B,i^0}, t_0\in T^0 \tag{33}$$

$$o_{h,i^0j,t_0,B} - (o_{h,i^0j_{i^0,E},t_0,E} + \sum_{j'\in U(i^0,j)} o_{h,i^0j',t_0,B}) \ge -M^4(1-\pi_{hi^0jt_0}),$$
$$\forall h\in H, i^0\in I^0, j\in J_{B,i^0}, t_0\in T^0 \tag{34}$$

Proof. The left side of Constraints (33) indicates the remaining available charging capacity at bus charging hub $j \in J_{B,i^0}$ if the charging demand of SMS zone $i^0 \in I^0$ is mandatorily assigned to this charging hub. If the left side of Constraints (33) does not exceed zero, bus charging hub $j \in J_{B,i^0}$ may fail to support the charging demand of SMS zone $i^0 \in I^0$. In this case, suppose that $\pi_{hi^0jt_0}$ can be zero or one. If $\pi_{hi^0jt_0}$ is zero, Constraint (34) is invalid. If $\pi_{hi^0jt_0}$ is one, Constraint (34) indicates that the charging demand of SMS zone $i^0 \in I^0$ must be met by bus charging hub $j \in J_{B,i^0}$. If that, however, it will violate Constraint (20). Therefore, $\pi_{hi^0jt_0}$ must be zero if the left side of constraints (33) is less than zero. If the left side of Constraints (33) is more than zero, $\pi_{hi^0jt_0}$ must be one. In this case, Constraint (34) ensures that the charging demand of SMS zone $i^0 \in I^0$ must be met by bus charging hub $j \in J_{B,i^0}$, implying that some feasible or optimal solutions for the current REHPP are excluded. According to Observation 1, Constraint (34) does not break the optimality of solutions to the follower problem. Therefore, Constraints (33) and (34) are super valid inequalities. □

Next, an example illustrates how to manually write Constraints (33) and (34). Suppose there is one SMS zone, one SMS charging point, and three bus charging hubs, as shown in Fig. 2. The operational costs are 10, 4, 5, and 6 for dispatching SMS batteries to SMS charging 1 and bus charging hubs 1, 2, and 3, respectively. We remove the indices of v, k, h, and t for simplicity. We use Q to represent the first two terms on the left side of Constraint (33). Then, Constraints (33) and (34) can be written as follows.

$$\begin{cases} Q_{j=1} - ed_{i^0=1} \le M^4\pi_{i^0=1,j=1} \\ Q_{j=2} - ed_{i^0=1} \le M^4\pi_{i^0=1,j=2} \\ Q_{j=3} - ed_{i^0=1} \le M^4\pi_{i^0=1,j=3} \end{cases} \tag{35}$$

$$\begin{cases} o_{i^0=1,j=1,B} - (o_{i^0=1,j=1,E} + \sum_{j\in\{2,3\}} o_{i^0=1,j',B}) \ge M^4(1-\pi_{i^0=1,j=1}) \\ o_{i^0=1,j=2,B} - (o_{i^0=1,j=1,E} + \sum_{j\in\{3\}} o_{i^0=1,j',B}) \ge M^4(1-\pi_{i^0=1,j=2}) \\ o_{i^0=1,j=3,B} - o_{i^0=1,j=1,E} \ge M^4(1-\pi_{i^0=1,j=3}) \end{cases} \tag{36}$$

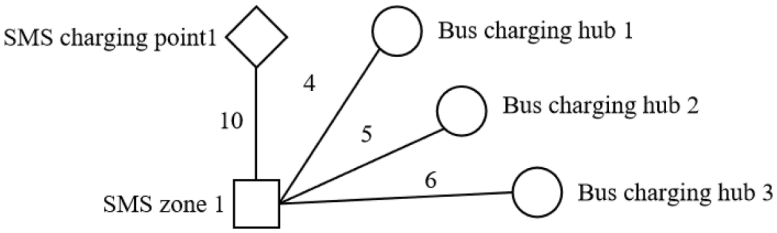

Fig. 2. An illustration of Constraints (33) and (34).

According to Constraints (35) and (36), suppose that $Q_j - ed_{i^0=1} > 0$ for $j = 1, 2, 3$. Then, $\pi_{i^0=1,j} = 1$ for $j = 1, 2, 3$. The optimal solution must be $o_{i^0=1,j=1,B} = 1$, $o_{i^0=1,j=1,E} = 0$, $o_{i^0=1,j=2,B} = 0$, and $o_{i^0=1,j=3,B} = 0$ because each SMS zone can be assigned to only one charging point or bus charging hub each time. Suppose that $Q_j - ed_{i^0=1} > 0$ for $j = 2$ and $Q_j - ed_{i^0=1} < 0$ for $j = 1, 3$. Then, the optimal solution must be $o_{i^0=1,j=1,B} = 0$, $o_{i^0=1,j=1,E} = 0$, $o_{i^0=1,j=2,B} = 1$, and $o_{i^0=1,j=3,B} = 0$. Suppose that $Q_j - ed_{i^0=1} < 0$ for $j = 1, 2, 3$. Then, the optimal solution must be $o_{i^0=1,j=1,B} = 0$, $o_{i^0=1,j=1,E} = 1$, $o_{i^0=1,j=2,B} = 0$, and $o_{i^0=1,j=3,B} = 0$.

5. Case study

This section presents a case study conducted in Gothenburg, Sweden, involving 70 bus routes, 705 buses, 61 bus terminals, and charging demands for over 12,000 e-scooters. Initially, we assess the algorithm's performance using numerical instances derived from this case study. Subsequently, we present the case study's results and evaluate them from PT operators, SMS operators, and sustainability.

5.1. Data collection

Västtrafik is the agency responsible for PT services, including buses, ferries, trains, and trams, in Gothenburg, Sweden (Wikipedia, 2024). The timetables of bus routes are available from Västtrafik's website (Västtrafik, 2024). We estimate the task-based electricity consumption of BEBs by considering their electricity consumption per kilometer and the length of each bus route. Here, we assume that the BEB electricity consumption per kilometer is 0.7 kWh (Doulgeris et al., 2024). Subsequently, we use a simulation-based approach to assign bus tasks to BEBs, ensuring the SoC for each bus remains between 20% and 100% without taking the charging capacity at bus terminals into account. In this step, we implement an opportunity-based charging strategy, where BEBs are charged at bus terminals between successive tasks. This process allows us to determine the specific task assignments for each BEB. Assume the maximum charging power of a charger is 450 kW and the BEB battery capacity is 300 kWh. The annual investment cost for a charger of 450 kW (C_{CH}) is US$5700 (Liu et al., 2021), and the annual investment for each kilowatt of installed solar PV capacity (C_{PV}) is US$25 (Liu et al., 2024). The service fee ranges from US$0 to US$2 for sensitivity analysis.

We divide the year into four seasons: spring, summer, autumn, and winter. The solar power outputs per kW in Gothenburg are collected for each season (ProfileSOLAR, 2024). The time-of-use electricity prices (Fig. 3) are obtained from the utility department in Gothenburg (NordPool, 2024). The average charging demand for an e-scooter battery is 0.63 kWh. The number of e-scooters requiring charging each hour in Gothenburg is derived from the transaction data of TIER and VOI. The e-scooter zones are divided based on user activity characteristics, as shown in Fig. 4. The sizes of the e-scooter zones are 500 m x 1000 m (red), 1000 m x 1000 m (orange), 2000 m x 2000 m (yellow), and 3000 m x 3000 m (blue). As Fig. 4 shows, we also assume there are four existing e-scooter charging points. The operational hourly cost of a battery dispatching trip includes both labor and electricity consumption costs and is calculated to be US$20.29 per hour in Sweden. Accordingly, the operational cost excluding service fee of an SMS battery dispatching trip from i to j is obtained by multiplying the trip duration by this hourly operational cost, assuming an average travel speed of 20 km/h. The maximum allowable installed capacity at a bus terminal can be determined by the available rooftop area of the surrounding buildings. Assuming each PV module occupies 1.62 m^2 and has a rated power of 0.327 kW (SunPower, 2017), the maximum capacity is obtained by calculating the number of modules that can be installed within the available area. The maximum number of chargers installed at a bus charging hub is set to 20. In Appendix B, we provide the detailed parameter settings and the case study setup.

5.2. Algorithm performance

We show the number of iterations and solution times of different numerical instances in Table 2 to evaluate the algorithm's performance. These instances are constructed using parameters from the case study. We adjust the number of bus routes and bus terminals included in the optimization model to vary the instance scales. Notably, the last instance corresponds to the scale of the case study. In Table 2, the 'Instance' column uses the notation 'xx-yy' to denote the inclusion of xx buses and yy bus terminals in the optimization model. As the number of buses and bus terminals increases, e-scooter operators have more options for scheduling battery charging, leading to an exponential increase in bi-level feasible solutions to the B-MILM. For the first five instances, the number of iterations is two, both with and without super-valid inequalities. This indicates that Algorithm 1 could reach the termination condition after only two iterations (including the initial solution-finding step). When the number of buses and bus terminals is small, the e-scooter operator has limited options for scheduling battery charging, and the PT operator has few opportunities to maximize benefits

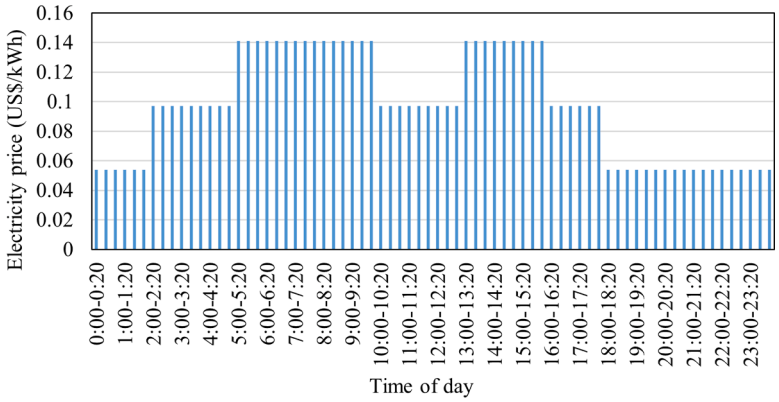

Fig. 3. The time-of-use electricity prices used in this case study.

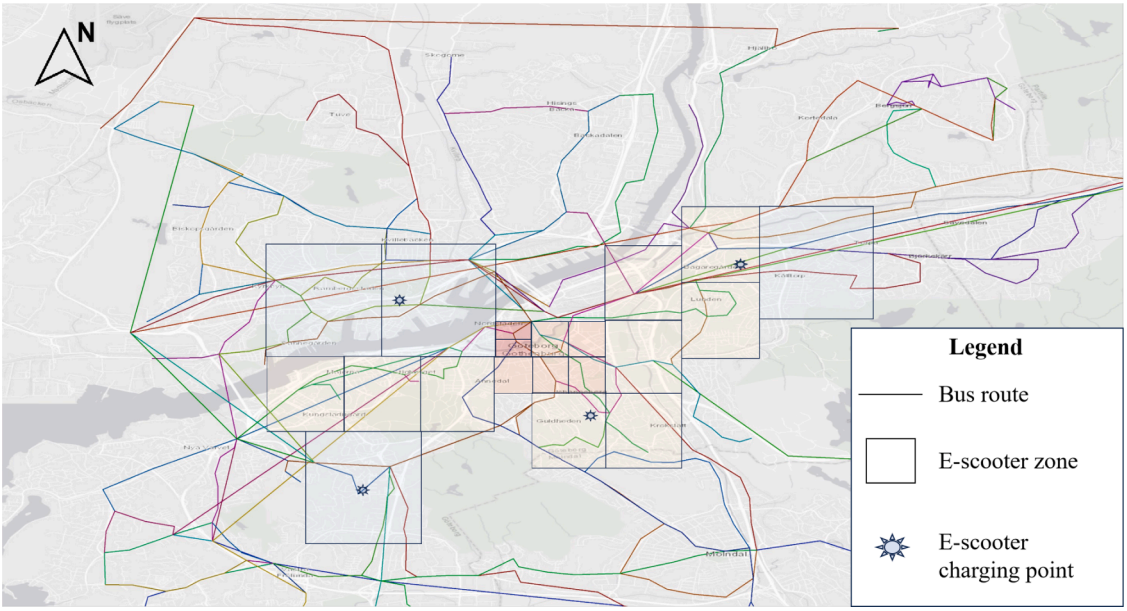

Fig. 4. E-scooter zones, charging points, and bus routes in this case study.

from the e-scooter operators. Consequently, Algorithm 1 can quickly reach the termination condition. For the first five instances, the solution time of the algorithm without super valid inequalities is shorter than with them because the super valid inequalities complicate model constraints, thereby requiring additional computational time for the solver when the number of iterations is the same. For the last seven instances, the number of iterations is two with super valid inequalities, while Algorithm 1 does not reach the termination condition within 86,400 seconds. The results of these numerical instances demonstrate that the algorithm incorporating super valid inequalities can effectively solve large-scale instances of the B-MILM. Table 3 shows the upper bound (UB), lower bound (LB), and optimality gap across different numerical instances. Under the imposed time limit, the optimality gap is at least 1% when the number of buses is 100 or more, if super valid inequalities are not used.

5.3. Economic impacts of solar PV and shared charging service

With the service fee set to zero, we compare the infrastructure investment and operational costs of PT and e-scooter operators under three scenarios: solar PV and shared charging service (Sharing + Solar PV), solar PV, and business as usual (BAU). Table 4 presents the economic impacts of solar PV and shared charging services on the PT operator. We calculate the investment efficiency under the Sharing + Solar PV and Solar PV scenarios as follows.

$$\text{Investment efficiency} = \frac{\text{Total cost}_{BAU} - \text{Total cost}_{s}}{\text{Infrastructure investment}_{s} - \text{Infrastructure investment}_{BAU}} \tag{37}$$

Table 2
Number of iterations and solution time of different numerical instances.

	With super valid inequalities		Without super valid inequalities	
Instances	Number of iterations	Time (s)	Number of iterations	Time (s)
10-2	2	608	2	417
20-2	2	642	2	379
30-4	2	657	2	532
40-6	2	841	2	598
50-6	2	571	2	639
100-11	2	1138	> 24	86,400
200-17	2	4096	> 20	86,400
300-25	2	8999	> 18	86,400
400-37	2	12,636	> 17	86,400
500-51	2	13,280	> 13	86,400
600-56	2	18,239	> 11	86,400
705-61	2	22,394	> 11	86,400

Table 3
Upper bound (UB), lower bound (LB), and optimality gap of different numerical instances.

	With super valid inequalities			Without super valid inequalities		
Instances	UB	LB	Gap	UB	LB	Gap
10–2	34,396	34,396	0%	34,396	34,396	0%
20–2	57,933	57,933	0%	57,933	57,933	0%
30–4	79,083	79,083	0%	79,083	79,083	0%
40–6	116,659	116,659	0%	116,659	116,659	0%
50–6	144,838	144,838	0%	144,838	144,838	0%
100–11	272,094	272,094	0%	272,891	272,007	0.3%
200–17	483,020	483,020	0%	485,121	482,402	0.6%
300–25	660,430	660,430	0%	666,702	659,758	1%
400–37	960,896	960,896	0%	968,675	959,084	1%
500–51	1,073,272	1,073,272	0%	1,082,146	1,071,432	1%
600–56	1,167,315	1,167,304	0.001%	1,178,587	1,165,436	1.1%
705–61	1,370,900	1,370,886	0.001%	1,382,656	1,368,967	1%

Table 4
Economic impacts of solar PV and shared charging service on the PT operator.

Annual cost	Sharing + Solar PV (US$)	Solar PV (US$)	BAU (US$)
Infrastructure investment	589,920	588,670	535,800
Operational cost	780,980	788,830	899,800
Total	1,370,900	1,377,500	1,435,600
Investment efficiency	120%	110%	NA

As shown in Table 4, the investment efficiency under the Sharing + Solar PV and Solar PV scenarios is 120% and 110%, respectively. Compared to the Solar PV scenario, the increased investment efficiency in the Sharing + Solar PV scenario is attributed to the increased electricity cost savings achieved by using solar PV power for charging SMS batteries. When the shared charging service is introduced, the infrastructure investment in solar PV installed capacity increases slightly. Compared to the BAU scenario, introducing solar PV can reduce operational costs (charging costs of BEBs) by substituting a portion of electricity purchases with solar-generated electricity. Notably, the utilization of solar PV remains consistent across all seasons, with nearly 100% utilization year-round. This suggests that energy storage deployment at bus charging hubs is unnecessary, as optimal solar PV deployment can maximize utilization without storage. Additionally, the current high cost of energy storage further supports this conclusion. For the e-scooter operator, introducing a shared charging service can reduce the annual operational costs (including electricity consumption for electric mini-trucks and labor costs) from $176,680 to $80,903, achieving a 54% reduction. In this case study, the number of location options for charging e-scooter batteries increases from 4 to 28 due to the introduction of the shared charging service mode.

We present the operational details of both the SMS and PT systems to explain the underlying reasons for these benefits further. Fig. 5 shows the number of SMS battery dispatching events from SMS zones to bus charging hubs and SMS charging points throughout the working hours of the day in Spring. 75.6% of the dispatching events are allocated to bus charging hubs to minimize trip costs. Fig. 6 illustrates the total charging demand of SMS batteries at bus charging hubs and SMS charging points.

Finally, we conduct a sensitivity analysis on the service fee, which ranges from US$0 to US$2. Under the sharing + Solar PV scenario, Fig. 7 shows the annual cost savings in SMS and PT systems as the service fee increases. In particular, the annual cost savings in PT are calculated by comparing the Solar PV scenario. The annual cost savings for PT show a nonlinear trend, while those for SMS exhibit a consistent downward trend. The maximum annual cost reduction for PT is US$45,441 when the service fee is

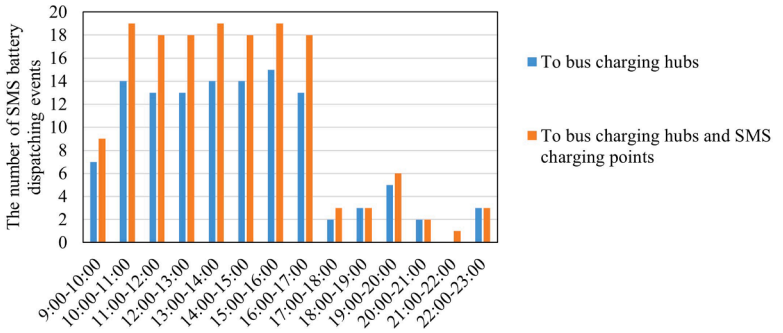

Fig. 5. The number of SMS battery dispatching events from SMS zones to bus charging hubs and SMS charging points.

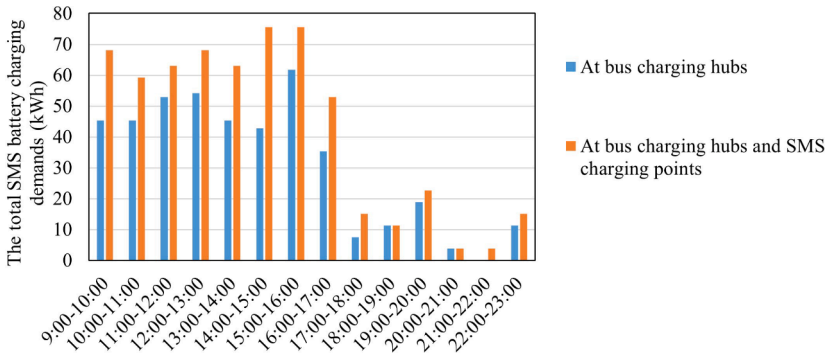

Fig. 6. The total SMS battery charging demands at bus charging hubs and SMS charging points.

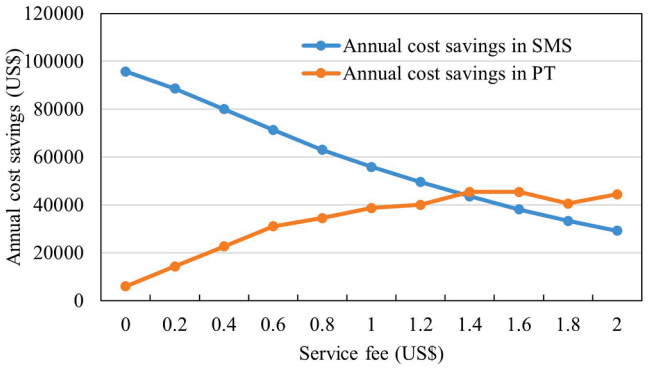

Fig. 7. The annual cost savings in SMS and PT.

US$1.4. The sensitivity analysis indicates that collaboration between SMS and PT can yield substantial benefits through the use of service fee signals as a control mechanism.

5.4. Impacts of solar PV on the grid

The impacts on the grid are primarily due to BEB charging, as the charging power and demand for e-scooter batteries are relatively minor. We compare the BEB charging demand and grid supply under the solar PV and BAU scenarios. Notably, under the BAU scenario, the BEB charging demand is entirely met by the grid, as no solar PV electricity is available. Fig. 8 depicts the daily BEB charging demand and grid load during spring, summer, autumn, and winter under the solar PV and BAU scenarios. In the BAU scenario, there is almost no BEB charging demand between 4:00 and 17:00 due to higher electricity prices (Fig. 3). Under the solar PV scenario, the distribution of BEB charging demands aligns with the distribution of solar PV generation. This is because shifting BEB charging demands from nighttime to daytime reduces charging costs by utilizing solar PV electricity. Compared to the BAU scenario, the net BEB charging loads on the grid decrease on average by 20%, 34%, 8%, and 3% in spring, summer, autumn, and winter, respectively. The results reveal that the seasonal impact of solar PV on the grid is obvious, corresponding to the varying solar PV power outputs in Gothenburg.

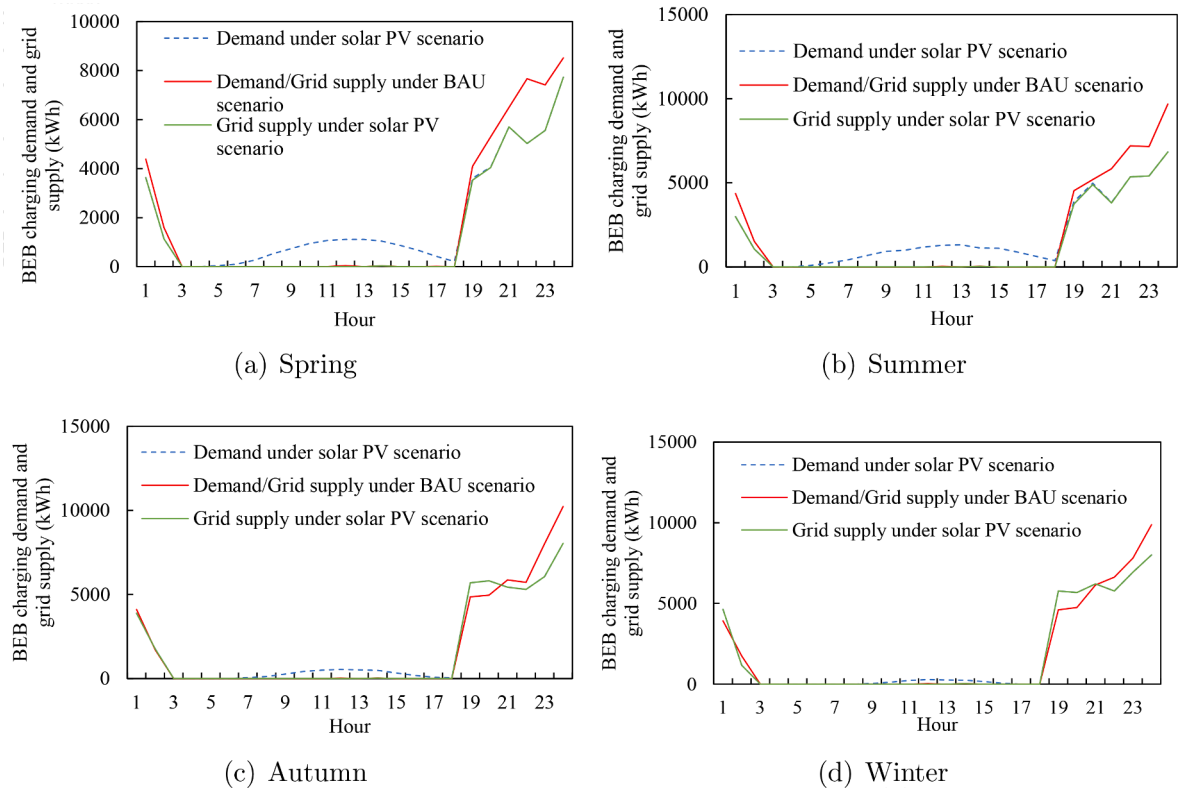

Fig. 8. Daily BEB charging demand and grid load in spring, summer, autumn, and winter.

Table 5
Number of chargers and installed capacity of solar PV under the three scenarios.

Charging infrastructure	Sharing + Solar PV	Solar PV	BAU
Number of chargers	94	94	94
Installed capacity of solar PV (kW)	2151	2101	NA

5.5. Impacts of solar PV and shared charging service on charging infrastructure planning

With the service fee set to zero, Table 5 presents the number of chargers and the installed capacity of solar PV under the three scenarios, illustrating the impacts of solar PV and shared charging services on charging infrastructure planning. The number of chargers required at bus charging hubs remains consistent across all three scenarios. Fig. 9 displays a histogram of the number of chargers deployed at bus charging hubs under each scenario. We find that 68% of bus terminals deploy one or zero chargers. Introducing solar PV at bus charging hubs alters the distribution of charging demands while keeping the total BEB charging demand unchanged. After implementing the shared charging service model, the investment in chargers does not increase, as the revenue from e-scooters does not offset the additional investment. However, the installed capacity of solar PV increases slightly under the shared charging service mode to boost revenue from e-scooters. Fig. 10 illustrates the spatial distribution of chargers and solar PV installations at bus terminals. The numbers indicate the required number of chargers at each terminal. Red and green colors represent the presence and absence of solar PV deployment, respectively. Finally, as the service fee increases, the total installed solar PV capacity exhibits only a slight variation, remaining within the range of 0–50 kW.

5.6. Impacts of solar PV on the greenhouse gas GHG emission

Battery-powered electric vehicles offer the advantage of zero emissions. However, the electricity consumed by these vehicles involves carbon emissions during its production and transmission. Although Sweden's power sector has the lowest greenhouse gas (GHG) emission intensity (8 gCO2e/kWh in 2022) in Europe (EuropeanEnvironmentAgency, 2024), the GHG intensity of electricity production differs significantly across different countries. We calculate the average value of GHG emission intensity of 28 countries in Europe is 253 gCO2e/kWh in 2022 (EuropeanEnvironmentAgency, 2024). We explore the impacts of solar PV on the GHG emissions for PT and shared e-scooter systems. The annual GHG emission is calculated on the basis of the total consumed electricity from the

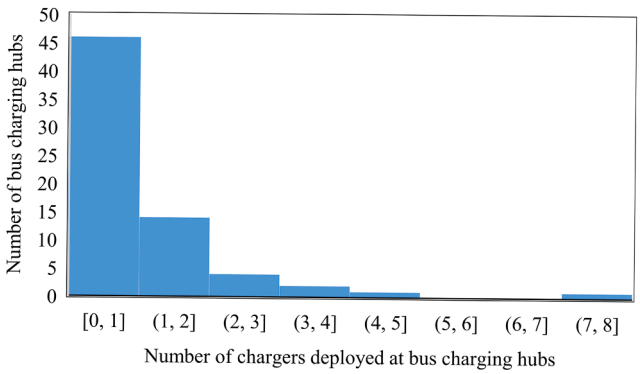

Fig. 9. The histogram of the number of chargers deployed at bus charging hubs under the three scenarios.

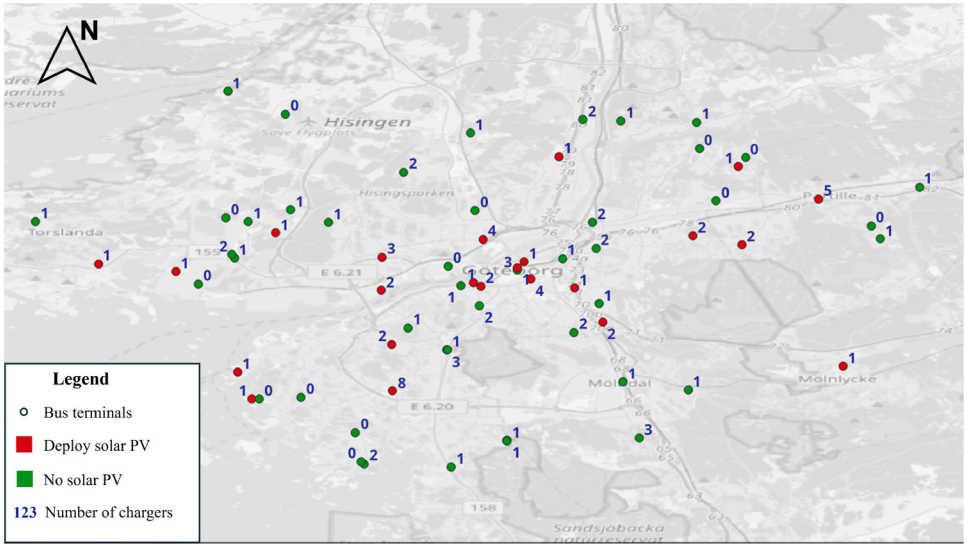

Fig. 10. The spatial distribution of chargers and solar PV at bus terminals.

Table 6
Number of chargers and installed capacity of solar PV under the three scenarios.

Annual GHG emission (t)	Sharing + Solar PV	Solar PV	BAU
PT and shared e-scooter systems	16,358	16,368	16,883

power grid and the corresponding GHG intensity of electricity production. Table 6 shows the annual GHG emissionsmodes of PT and shared e-scooter systems under the three scenarios. Under the BAU scenario, the annual GHG emissions of PT and shared e-scooter systems amount to 16,883 t. Introducing solar PV reduces the annual GHG emissions by 515 t (3%). Furthermore, implementing the shared charging service model reduces the annual GHG emissions by an additional 10 t compared to the Solar PV scenario.

6. Discussion and conclusions

This study presents a bus charging infrastructure planning problem incorporating shared micromobility and the adoption of solar photovoltaic. The purpose is to mitigate the adverse effects of rapid transportation electrification in urban areas, such as grid load, low charging service efficiency, and the limited mobility of shared micro-mobility systems, by highlighting the introduction of solar photovoltaic and shared charging service mode. The problem is formulated as a bi-level mixed-integer linear programming model to address the differing interests and interactive decision-making processes. To tackle the computational challenges, particularly for city-scale instances, we employ a value-function-based approach incorporating super valid inequalities. The super valid inequalities handle the necessary condition of the optimal solutions to shared micromobility operators. We add the super valid inequalities into the restricted extended high point problem during the iteration-based algorithm to accelerate the algorithm convergence speed.

Numerical results demonstrate that leveraging super valid inequalities reduces solution time by at least 98% for the large-scale instances. Our proposed optimization model and solution approaches can be applied to various shared micromobility systems, such as the e-scooters investigated in the case study, e-bikes, and even e-freight systems. In these shared micromobility or e-freight systems, charging demand can be inferred from transaction or operational data. The constraints of follower problems can be slightly adjusted to accommodate different scenarios. However, the objective of follower problems remains consistent: to minimize the charging dispatching costs between service zones and charging infrastructure. Therefore, similar super valid inequalities can be derived via the idea in this study.

The case study demonstrates our proposed optimization model at the city level using 70 bus routes, 705 buses, 61 bus terminals, and charging demands for over 12,000 e-scooters in Gothenburg, Sweden. The economic benefits of solar photovoltaic are evident, and the investment efficiency ranges between 110% and 120%, even when the service fee is excluded. Notably, this study does not integrate energy storage into solar photovoltaic because it is necessary to understand the economic benefits of solar photovoltaic without energy storage under the current high investment costs of energy storage. However, our model can be easily extended to include energy storage considerations. In general, the shared charging service offers greater economic benefits for shared e-scooter operators than for public transport operators, given the service fee ranging from US$0 to US$2. It can achieve up to 54% reduction in electricity consumption for electric mini-trucks and labor costs for the e-scooter operators. Opening bus charging hubs to e-scooter operators provides them with more charging location options and reduces dispatching distances. Consequently, this integration not only lowers operational costs for e-scooter operators but also ensures timely and sufficient battery power for e-scooters, enhancing e-scooter mobility. Integrating solar photovoltaic can reduce daily grid loads for electric bus charging by 3% to 34% across different seasons. This significant seasonal impact corresponds to the varying solar photovoltaic power outputs in Gothenburg. Compared with existing studies (Liu et al., 2024; Ren et al., 2022), we find that the characteristics of solar resources in different countries and regions significantly influence grid performance. Under the average greenhouse gas emission intensity in Europe, introducing solar photovoltaic reduces annual greenhouse gas emissions by 3%. Integrating a shared charging service further increases this reduction to 3.1%.

Future research can extend the current study in two key areas. First, dynamic electricity markets and infrastructure resilience affected by climate change should be considered at the planning stage. Second, the vehicle routing problem of shared micromobility systems can be integrated into the joint charging scheduling optimization for electric buses and shared micromobility vehicles.

CRediT authorship contribution statement

Xiaohan Liu: Writing – original draft, Visualization, Software, Methodology, Investigation, Conceptualization; **Arsalan Najafi:** Methodology, Investigation; **Sheng Jin:** Writing – review & editing, Visualization, Validation; **Hua Wang:** Writing – review & editing, Visualization, Validation; **Xiaolei Ma:** Writing – review & editing, Visualization, Validation; **Kun Gao:** Writing – review & editing, Validation, Supervision, Funding acquisition, Conceptualization.

Data availability

Data will be made available on request.

Declaration of competing interest

The authors declare that they have no known competing financial interests or personal relationships that could have appeared to influence the contents in this paper.

Acknowledgments

The research is funded by JPI Urban Europe and Energimyndigheten (e-MATS, P2023-00029) and supported by Area of Advance Transport at Chalmers University of Technology. The research is also supported by National Natural Science Foundation Council of China (Grant No. 72471070), Beijing Nova Program (No. 20230484432) amd Beijing Natural Science Foundation (No. JQ24051). Any opinions, findings, conclusions or recommendations expressed in this paper are those of the authors and do not necessarily reflect the sponsors' views.

Appendix A. The description of EHPP

First, we define a generalized bi-level program as follows. Notably, the mathematical notation used in this appendix is independent of that in the main text.

$$z^* = \min_{(x,y)} \phi^l(x, y) \tag{A.1}$$

$$x \geq 0, x \in \mathbb{Z} \tag{A.2}$$

$$g_j^1(x) + h_j^1(y) \leq b_j^1, \forall j = 1, \ldots, m_1 \tag{A.3}$$

$$y \in \arg\min_{y^f}\{\phi^l(x, y^f) | g_j^2(x) + h_j^2(y^f) \le b_j^2, \forall j = 1, \dots, m_2, y^f \ge 0, y^f \in \mathbb{Z}\} \tag{A.4}$$

Here, $\phi^l(x, y)$ is the objective function of the leader problem, where x presents the leader variables and y denotes the optimal follower variables given x. x and y are non-negative integers. But we have shown that, in our problem, it suffices to require that the leader variables appearing in the follower problem are non-negative integers, which guarantees convergence (see Proposition 1). Constraint (A.3) is the constraint for the leader problem. Eq. (A.4) presents the optimal solution of y^f given x. Actually, Eq. (A.4) indicates the follower problem. $g_j^2(x) + h_j^2(y^f) \le b_j^2$ is the follower constraint.

The corresponding HPP is formulated as follows.

$$z^{HPP} = \min_{(x,y)\in\Omega} \phi^l(x, y) \tag{A.5}$$

Where x and y represent the leader and follower variables, respectively. Let Ω denote the set of all feasible (x, y) satisfying the defined original constraints. In the HPP, the follower's optimality is relaxed, and the corresponding constraints are incorporated into the leader problem, thereby converting the bi-level formulation into a single-level problem. We do not have to ensure y is optimal given the x in the HPP, so z^{HPP} must be a lower bound for z^*.

To give the EHPP, we first introduce the following propositions.

Proposition A1 (Lozano and Smith, 2017). *Let Y denote the set of feasible follower variables related to all feasible leader variables. Define $\gamma_{\hat{y},j} = \lfloor b_j^2 - h_j^2(\hat{y}) \rfloor + 1$ for every $\hat{y} \in Y, j = 1, \dots, m_2$. Here, $\lfloor\rfloor$ is the floor operator, and it rounds a value down to the nearest integer. The leader blocks the solution $\hat{y} \in Y$ by constraint j if and only if $g_j^2(x) \ge \gamma_{\hat{y},j}$.*

Proposition A2 (Lozano and Smith, 2017). *Define $B(\hat{y}, Y) = \{(y', q) | \gamma_{y',q} \ge \gamma_{\hat{y},q}, y' \in Y, q = 1, \dots, m_2\}$. This set represents all ordered pairs (y', q), such that if x blocks $y' \in Y$ by constraint q, then x also blocks $\hat{y}$ by constraint q.*

Then, the EHPP can be formulated as follows.

$$\min_{(x,y)} \phi^l(x, y) \tag{A.6}$$

$$g_j^2(x) \ge -M_j^1 + \sum_{\hat{y}\in Y} (M_j^1 + \gamma_{\hat{y},j})\omega_{\hat{y},j}, \forall j = 1, \dots, m_2 \tag{A.7}$$

$$\phi^f(x, y) \le \phi^f(x, \hat{y}) + M_{\hat{y}}^2 \sum_{(y',q)\in B(\hat{y},Y)} \omega_{y',q}, \forall \hat{y} \in Y \tag{A.8}$$

$$(x, y) \in \Omega \tag{A.9}$$

$$\omega_{\hat{y},j} \in \{0, 1\}, \hat{y} \in Y, j = 1, \dots, m_2 \tag{A.10}$$

Where M_j^1 and $M_{\hat{y}}^2$ sufficiently large numbers. $\phi^f(x, y)$ denote the objective function of the follower problem. Let $\omega_{\hat{y},j}$ denote a binary variable: 1 if constraint j blocks $\hat{y}$, otherwise 0. Let Ω denote the set of all feasible (x, y) satisfying the defined original constraints. Next, the following proposition shows that the EHPP is equivalent to the generalized bi-level program.

Proposition A3 (Lozano and Smith, 2017). *The EHPP is equivalent to the generalized bi-level program.*

Now, we return to the problem considered in this study. Clearly, the proposed formulation is a bi-level program that satisfies the conditions required to transform it into the EHPP. Moreover, we have shown that it suffices to require the leader variables appearing in the follower problem to be non-negative integers, which guarantees convergence (see Proposition 1).

Appendix B. Case study setup

Table B.7 presents key parameters and data sources for the case study. The BEB energy consumption for a given trip is estimated as the product of the energy consumption rate and the trip distance. Trip distances are obtained from the website reporting bus routes and timetables in Gothenburg. Given the installed PV capacity, the solar PV power output is estimated by multiplying the hourly PV output per unit of installed capacity by the installed capacity. In Gothenburg, the hourly PV output per unit capacity is provided as four seasonal profiles corresponding to the four seasons of the year. Given the maximum available area for deploying PV panels at bus charging hubs, we compute the maximum installable PV capacity based on the rated power and footprint area of the PV modules. Based on the bus routes and timetables in Gothenburg, we identify the relationships between routes and bus terminals and construct the corresponding bus network.

Table B.7
Key parameters and data sources for the case study.

Parameters	Values	Explanation
Number of SMS zones	20	500 m × 1000 m: 2; 1000 m × 1000 m: 5; 2000 m × 2000 m: 9; 3000 m × 3000 m: 4
Number of SMS batteries needing to be charged	See Appendix C	Per hour per zone.
Averaged charging demand of an SMS battery	0.63 kWh	Data source: https://www.ewheels.se/elsparkcykel/e2s-urban-max/?code=10916.
BEB energy consumption rate	0.7 kWh/km	(Doulgeris et al., 2024).
BEB energy consumption per trip	0.7× (trip distance)	Computed as (energy consumption rate) × (trip distance).
BEB battery capacity	300 kWh	
BEB charging power	450 kW	
Annual investment cost of a charger	US$5,700	(Liu et al., 2021).
Annual investment cost of solar PV	US$25/kW	(Liu et al., 2024).
Hourly PV power outputs per kW	See the website	Retrieved from https://profilesolar.com/locations/Sweden/Gothenburg/.
Hourly PV power outputs	(Installed PV capacity)×(Hourly PV output per kW)	Computed as installed PV capacity multiplied by hourly PV output per kW.
Maximum number of chargers installed at a bus charging hub	20	
PV module area	1.62 m^2	(SunPower, 2017).
Rated power of a PV module	0.327 kW	(SunPower, 2017).
Maximum area for deploying PV panels at bus charging hubs	–	Obtained from Google Maps.
Current bus routes and timetables	See the website	(Västtrafik, 2024).
Time-of-use electricity price	See Fig. 3	(NordPool, 2024).
Travel speed of electric trucks carrying SMS batteries	20 km/h	
Operational hourly cost of a battery dispatching trip	US$20.2948/hour	Including both labor and electricity consumption costs. Data source: https://www.salaryexpert.com/salary/job/video-editor/sweden.

Appendix C. Number of SMS batteries needing to be charged

Table C.8 presents the number of SMS batteries needing to be charged per hour per zone. The column of Zone_ID represents the ID of SMS zones. The columns of H1–H24 present the hour index.

Table C.8
Number of SMS batteries needing to be charged.

Zone ID	H1	H2	H3	H4	H5	H6	H7	H8	H9	H10	H11	H12	H13	H14	H15	H16	H17	H18	H19	H20	H21	H22	H23	H24
1	0	0	0	0	0	0	0	0	0	12	2	2	2	8	2	2	2	0	0	0	0	0	0	0
2	0	0	0	0	0	0	0	0	0	6	6	6	12	6	6	12	6	0	0	0	0	0	0	0
3	0	0	0	0	0	0	0	0	0	24	10	4	4	10	22	10	4	12	0	6	0	0	0	0
4	0	0	0	0	0	0	0	0	0	0	6	12	6	6	6	18	6	0	0	0	0	0	6	0
5	0	0	0	0	0	0	0	0	0	6	2	2	2	2	2	8	2	0	0	0	0	0	0	0
6	0	0	0	0	0	0	0	0	0	6	6	12	6	12	12	6	12	0	0	0	0	0	0	0
7	0	0	0	0	0	0	0	0	0	6	6	12	12	12	12	6	6	0	6	6	0	0	0	0
8	0	0	0	0	0	0	0	0	0	0	6	6	12	6	6	6	6	0	0	0	0	6	0	0
9	0	0	0	0	0	0	0	0	0	0	2	8	2	2	2	2	2	0	0	0	0	0	0	0
10	0	0	0	0	0	0	0	0	0	24	6	6	6	6	6	12	12	0	0	6	0	0	0	0
11	0	0	0	0	0	0	0	0	0	6	0	0	0	6	0	6	0	0	0	6	0	0	0	0
12	0	0	0	0	0	0	0	0	0	0	6	6	12	6	12	12	6	6	0	6	0	0	6	0
13	0	0	0	0	0	0	0	0	0	0	4	4	4	4	10	4	4	0	0	0	0	0	0	0
14	0	0	0	0	0	0	0	0	0	0	8	2	2	2	2	2	2	0	0	0	0	0	0	0
15	0	0	0	0	0	0	0	0	0	0	2	2	2	2	2	8	2	0	6	0	0	0	0	0
16	0	0	0	0	0	0	0	0	0	0	2	2	2	2	2	2	2	6	6	0	0	0	6	0
17	0	0	0	0	0	0	0	0	0	18	8	8	8	2	2	2	2	0	0	0	0	0	0	0
18	0	0	0	0	0	0	0	0	0	0	6	0	0	0	0	0	0	0	0	6	0	0	0	0
19	0	0	0	0	0	0	0	0	0	0	4	4	13	4	1	1	1	0	0	0	3	0	0	0
20	0	0	0	0	0	0	0	0	0	0	4	4	13	4	1	1	1	0	0	0	3	0	0	0

Appendix D. An example to illustrate the algorithm

We present an illustrative example of the proposed algorithm. We consider an instance with 100 buses and 11 bus terminals. Table D.9 reports the solution statistics across iterations, including the UB, LB, the follower objective value in the REHPP, and the optimal follower objective (given the leader decisions). In the first iteration, the algorithm has not converged, as indicated by a nonzero UB–LB gap and by the discrepancy between the follower objective in the REHPP and its optimal value under the corresponding leader decisions. The discrepancy between the follower objective in the REHPP and its optimal value under the corresponding leader decisions indicates that the current REHPP does not satisfy bi-level optimality, as it violates the follower's optimality condition. In contrast, in the second iteration, with the aid of the super valid inequalities and the added cutting-plane constraints, the follower optimality condition is enforced, and bi-level optimality is achieved.

Fig. D.11 shows the cumulative number of battery dispatching events between the SMS zones and bus charging hubs in the first and second iterations. The follower decisions differ markedly between the two iterations. After the second iteration, the follower decisions reach the optimal solution, enabled by the super valid inequalities and the added cutting-plane constraints.

Table D.9
Solution statistics across iterations.

Iteration	UB	LB	Follower objective value in the REHPP	Optimal follower objective
1	273,102	271,974	135,153	116,267
2	272,094	272,094	119,246	119,246

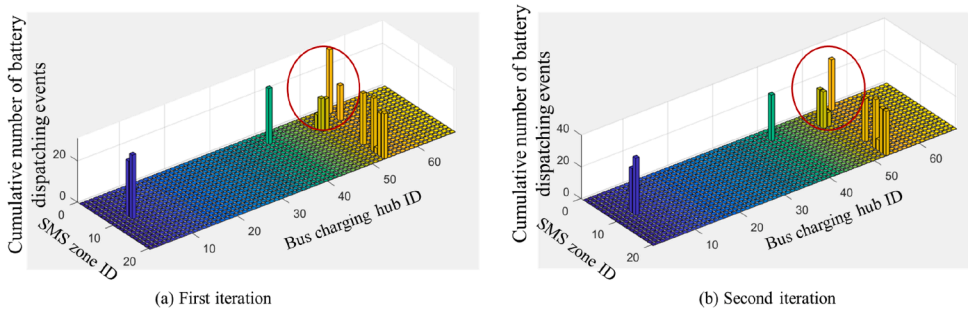

(a) First iteration (b) Second iteration

Fig. D.11. Cumulative number of battery dispatching events between the SMS zones and bus charging hubs in the first and second iterations.

References

Abdelwahed, A., van den Berg, P.L., Brandt, T., Collins, J., Ketter, W., 2020. Evaluating and optimizing opportunity fast-charging schedules in transit battery electric bus networks. Transp. Sci. 54 (6), 1601–1615.

Alwesabi, Y., Avishan, F., Yanłkoğlu, I., Liu, Z., Wang, Y., 2022. Robust strategic planning of dynamic wireless charging infrastructure for electric buses. Appl. Energy 307, 118243. https://doi.org/10.1016/j.apenergy.2021.118243

Cai, Z., Li, C., Mo, D., Xu, S., Chen, X.M., Lee, D.-H., 2024. Optimizing consolidated shared charging and electric ride-sourcing services. Transp. Res. Part E: Logist. Transp. Rev. 184, 103484. https://doi.org/10.1016/j.tre.2024.103484

Caustur, L., Hertoghe, P., Ma, T.-Y., Vandebroek, M., 2025. Integrated charging scheduling for electric buses with time-of-use tariffs, peak power, v2g, battery ageing, and renewables. arXiv preprint arXiv:2509.05940 .

Cui, S., Gao, K., Yu, B., Ma, Z., Najafi, A., 2023. Joint optimal vehicle and recharging scheduling for mixed bus fleets under limited chargers. Transp. Res. Part E: Logist. Transp. Rev. 180, 103335. https://doi.org/10.1016/j.tre.2023.103335

Doulgeris, S., Zafeiriadis, A., Athanasopoulos, N., Tzivelou, N., Michali, M.E., Papagianni, S., Samaras, Z., 2024. Evaluation of energy consumption and electric range of battery electric buses for application to public transportation. Transp. Eng. 15, 100223. https://doi.org/10.1016/j.treng.2023.100223

Esmaeilnejad, S., Kattan, L., Wirasinghe, S.C., 2023. Optimal charging station locations and durations for a transit route with battery-electric buses: a two-stage stochastic programming approach with consideration of weather conditions. Transp. Res. Part C: Emerg. Technol. 156, 104327. https://doi.org/10.1016/j.trc.2023.104327

EuropeanEnvironmentAgency, 2024. Greenhouse gas emission intensity of electricity generation in Europe. https://www.eea.europa.eu/en/analysis/indicators.

Foda, A., Abdelaty, H., Mohamed, M., El-Saadany, E., 2023. A generic cost-utility-emission optimization for electric bus transit infrastructure planning and charging scheduling. Energy 277, 127592. https://doi.org/10.1016/j.energy.2023.127592

He, Y., Liu, Z., Song, Z., 2022. Integrated charging infrastructure planning and charging scheduling for battery electric bus systems. Transp. Res. Part D: Transp. Environ. 111, 103437. https://doi.org/10.1016/j.trd.2022.103437

He, Z., Yang, Y., Mu, Y., Qu, X., 2025. Public acceptance of driverless buses: An extended UTAUT2 model with anthropomorphic perception and empathy. Commun. Transp. Res. 5, 100167. https://doi.org/10.1016/j.commtr.2025.100167

Huang, D., Zhang, J., Liu, Z., 2023. A robust coordinated charging scheduling approach for hybrid electric bus charging systems. Transp. Res. Part D: Transp. Environ. 125, 103955. https://doi.org/10.1016/j.trd.2023.103955

IEA, 2024. Global EV outlook 2023. https://www.iea.org/reports/global-ev-outlook-2023.

Ji, J., Bie, Y., Wang, L., 2023. Optimal electric bus fleet scheduling for a route with charging facility sharing. Transp. Res. Part C: Emerg. Technol. 147, 104010. https://doi.org/10.1016/j.trc.2022.104010

Jia, Z., An, K., Ma, W., 2024. Utilizing electric bus depots for public charging: operation strategies and benefit analysis. Transp. Res. Part D: Transp. Environ. 130, 104155. https://doi.org/10.1016/j.trd.2024.104155

Lee, G., Lee, J.S., Park, K.S., 2024. Battery swapping, vehicle rebalancing, and staff routing for electric scooter sharing systems. Transp. Res. Part E: Logist. Transp. Rev. 186, 103540. https://doi.org/10.1016/j.tre.2024.103540
Levy, 2024. Electric shared scooters: How do they get recharged? https://www.levyelectric.com/.
Li, A., Gao, K., Zhao, P., Axhausen, K.W., 2024a. Integrating shared e-scooters as the feeder to public transit: a comparative analysis of 124 european cities. Transp. Res. Part C: Emerg. Technol. 160, 104496. https://doi.org/10.1016/j.trc.2024.104496
Li, L., Lo, H.K., Huang, W., Xiao, F., 2021. Mixed bus fleet location-routing-scheduling under range uncertainty. Transp. Res. Part B: Methodol. 146, 155–179. https://doi.org/10.1016/j.trb.2021.02.005
Li, W., He, Y., Hu, S., He, Z., Ratti, C., 2024b. Planning dynamic wireless charging infrastructure for battery electric bus systems with the joint optimization of charging scheduling. Transp. Res. Part C: Emerg. Technol. 159, 104469. https://doi.org/10.1016/j.trc.2023.104469
Liu, X., Cathy Liu, X., Liu, Z., Shi, R., Ma, X., 2023a. A solar-powered bus charging infrastructure location problem under charging service degradation. Transp. Res. Part D: Transp. Environ. 119, 103770. https://doi.org/10.1016/j.trd.2023.103770
Liu, X., Liu, X., Zhang, X., Zhou, Y., Chen, J., Ma, X., 2023b. Optimal location planning of electric bus charging stations with integrated photovoltaic and energy storage system. Comput.-Aided Civ. Infrastruct. Eng. 38 (11), 1424–1446. https://doi.org/10.1111/mice.12935
Liu, X., Plötz, P., Yeh, S., Liu, Z., Liu, X.C., Ma, X., 2024. Transforming public transport depots into profitable energy hubs. Nat. Energy 9, 1206–1219. https://doi.org/10.1038/s41560-024-01580-0
Liu, X., Qu, X., Ma, X., 2021. Optimizing electric bus charging infrastructure considering power matching and seasonality. Transp. Res. Part D: Transp. Environ. 100, 103057. https://doi.org/10.1016/j.trd.2021.103057
Lozano, L., Smith, J.C., 2017. A value-function-based exact approach for the bilevel mixed-integer programming problem. Oper. Res. 65 (3), 768–786. https://doi.org/10.1287/opre.2017.1589
Luo, Y., Zeng, B., Zhang, W., Liu, Y., Shi, Q., Liu, W., 2024. Coordinative planning of public transport electrification, RESs and energy networks for decarbonization of urban multi-energy systems: a government-market dual-driven framework. IEEE Trans. Sustain. Energy 15 (1), 538–555. https://doi.org/10.1109/TSTE.2023.3306912
Mahyari, E., Freeman, N., Yavuz, M., 2023. Combining predictive and prescriptive techniques for optimizing electric vehicle fleet charging. Transp. Res. Part C: Emerg. Technol. 152, 104149. https://doi.org/10.1016/j.trc.2023.104149
McCabe, D., Ban, X., Kulcsár, B., 2025. Minimum-delay opportunity charging scheduling for electric buses. Commun. Transp. Res. 5, 100209. https://doi.org/10.1016/j.commtr.2025.100209
MMfE, 2023. Technical requirements for e-scooters. https://micromobilityforeurope.eu/technical-requirements-for-e-scooters/.
NACTO, 2020. Shared micromobility in the US: 2019. https://nacto.org/shared-micromobility-2019/.
Nath, R.B., Rambha, T., Schiffer, M., 2024. On the impact of co-optimizing station locations, trip assignment, and charging schedules for electric buses. Transp. Res. Part C: Emerg. Technol. 167, 104839. https://doi.org/10.1016/j.trc.2024.104839
NordPool, 2024. Prices. https://www.nordpoolgroup.com/en/.
Osorio, J., Lei, C., Ouyang, Y., 2021. Optimal rebalancing and on-board charging of shared electric scooters. Transp. Res. Part B: Methodol. 147, 197–219. https://doi.org/10.1016/j.trb.2021.03.009
ProfileSOLAR, 2024. Solar PV analysis of gothenburg, sweden. https://profilesolar.com/locations/Sweden/Gothenburg/.
Ren, H., Ma, Z., Fai Norman Tse, C., Sun, Y., 2022. Optimal control of solar-powered electric bus networks with improved renewable energy on-site consumption and reduced grid dependence. Appl. Energy 323, 119643. https://doi.org/10.1016/j.apenergy.2022.119643
Shared micromobility, 2021. How to feed a hungry scooter. https://shared-micromobility.com/articles-all/.
SunPower, 2017. Sunpower e-series commercial solar panels e-20-327-com. https://energosave.pro/storage/products-xls/1613568296602d1928be3700.63763184.pdf.
Västtrafik, 2024. Timetables. https://www.vasttrafik.se/en/travel-planning/Timetables/.
Wang, X., Song, Z., Xu, H., Wang, H., 2023. En-route fast charging infrastructure planning and scheduling for battery electric bus systems. Transp. Res. Part D: Transp. Environ. 117, 103659. https://doi.org/10.1016/j.trd.2023.103659
Wang, Y., Zhou, Y., Yan, X., 2024. Reliable dynamic wireless charging infrastructure deployment problem for public transport services. Eur. J. Oper. Res. 313 (2), 747–766. https://doi.org/10.1016/j.ejor.2023.08.053
Wikipedia, 2024. Västtrafik. https://sv.wikipedia.org/wiki/V%C3%A4sttrafik.
Zhang, L., Liu, Z., Wang, W., Yu, B., 2022. Long-term charging infrastructure deployment and bus fleet transition considering seasonal differences. Transp. Res. Part D: Transp. Environ. 111, 103429. https://doi.org/10.1016/j.trd.2022.103429
Zhou, Y., Meng, Q., Ong, G.P., 2022a. Electric bus charging scheduling for a single public transport route considering nonlinear charging profile and battery degradation effect. Transp. Res. Part B: Methodol. 159, 49–75. https://doi.org/10.1016/j.trb.2022.03.002
Zhou, Y., Ong, G.P., Meng, Q., Cui, H., 2023. Electric bus charging facility planning with uncertainties: model formulation and algorithm design. Transp. Res. Part C: Emerg. Technol. 150, 104108. https://doi.org/10.1016/j.trc.2023.104108
Zhou, Y., Wang, H., Wang, Y., Li, R., 2022b. Robust optimization for integrated planning of electric-bus charger deployment and charging scheduling. Transp. Res. Part D: Transp. Environ. 110, 103410. https://doi.org/10.1016/j.trd.2022.103410